ACS OMEGA

Open Access

http://pubs.acs.org/journal/acsodf

Article

Graphene Pseudoreference Electrode for the Development of a Practical Paper-Based Electrochemical Heavy Metal Sensor

Prasongporn Ruengpirasiri, Pimchanok Charoensin, Akkrawat Aniwattapong, Pemika Natekuekool, Chawin Srisomwat, Chanika Pinyorospathum, Sudkate Chaiyo, and Abdulhadee Yakoh*

Cite This: *ACS Omega* 2024, 9, 1634−1642

Read Online

ACCESS | Metrics & More | Article Recommendations | Supporting Information

ABSTRACT: Paper-based electrochemical devices (PEDs) have emerged as versatile platforms that bridge analytical chemistry and materials science, demonstrating advantages of portability, cost-effectiveness, and environmental sustainability. This study investigates the integration of a graphene pseudoreference electrode (GPRE) into a PED, and it exhibits potential advantages over the traditional Ag/AgCl pseudoreference electrode (PRE). In addition, the electrochemical properties and stability of GPRE are compared with those of the traditional Ag/AgCl PRE. The results demonstrate that GPRE exhibits a stable and reproducible potential during electrochemical measurement throughout 180 days, demonstrating its suitability as an alternative to an expensive metal PRE. Furthermore, a GPRE-incorporated paper-based device is designed and evaluated for use in the electrochemical detection of cadmium (Cd) and lead (Pb) using an in situ bismuth-modified electrode. The GPRE-incorporated PED exhibited good analytical performance, with a low limit of detection of 0.69 and 5.77 ng mL^{-1} and electrochemical sensitivities of 70.16 and 38.34 $\mu A \cdot mL \cdot \mu g^{-1} \cdot cm^{-2}$ for Cd(II) and Pb(II), respectively. More than 99.9% accuracy of the sensor was obtained for both ions with respect to conventional inductively coupled plasma-mass spectrometry. The results highlight the effectiveness and suitability of the GPRE-incorporated PED as a sensor for various applications, such as environmental monitoring, food quality control, and medical diagnostics.

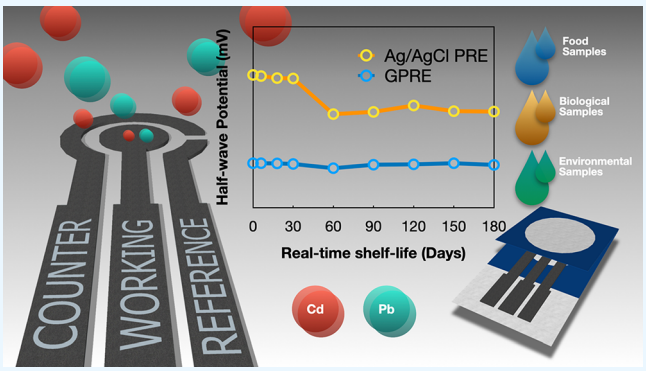

1. INTRODUCTION

Paper-based electrochemical devices (PEDs) have emerged as a versatile and innovative platform that bridges analytical chemistry and material science.[1,2] By integration of the inherent characteristic properties of paper with electrochemical principles, PEDs provide portable, inexpensive, and environmentally sustainable solutions for diverse applications. Moreover, owing to their disposability, these devices have garnered recognition as a safer alternative for detecting toxic compounds such as pathogens, contaminants, and heavy metals, thereby minimizing postuse environmental impact.[3−5]

Meanwhile, screen printing is frequently employed to fabricate the majority of PED electrodes, enabling diverse electrode configurations.[6,7] Electrodes—comprising a working electrode (WE), counter electrode (CE), and reference electrode (RE)—can be printed onto substrates via a process known as thick-film deposition,[8] in which conductive materials are compressed through a mesh screen[9] and dried under hot air. Inks or pastes are commonly made of carbon (e.g., carbon black, graphite, etc.) or metallic forms such as gold, silver, and platinum.[10] Various carbon-based materials, including graphene and its derivatives,[11−14] are often used as WE and CE because they possess exceptional features in electrochemistry including high conductivity and low background current. Moreover, the inks allow plenty of simple surface modifications such as metal depositions and composites self-assembling, which promote the sensitivity and selectivity of detection while providing simplicity of fabrication and importantly contributing to lower prices. Frequently, a silver/silver chloride (Ag/AgCl)[15] is applied as the paste for RE; it serves as a pseudoreference electrode (PRE) that simulates the behavior of an actual RE—a silver wire coated with AgCl immersed in a saturated chloride-containing solution.[16,17] Despite the widespread use of Ag/AgCl PRE, challenges persist. It exhibits shifts in potential due to interactions with ions during experiments, causing inaccuracies—especially in dynamic environments.[16] Furthermore, as the AgCl layer undergoes

Received: October 20, 2023
Revised: November 23, 2023
Accepted: November 29, 2023
Published: December 20, 2023

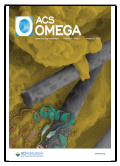

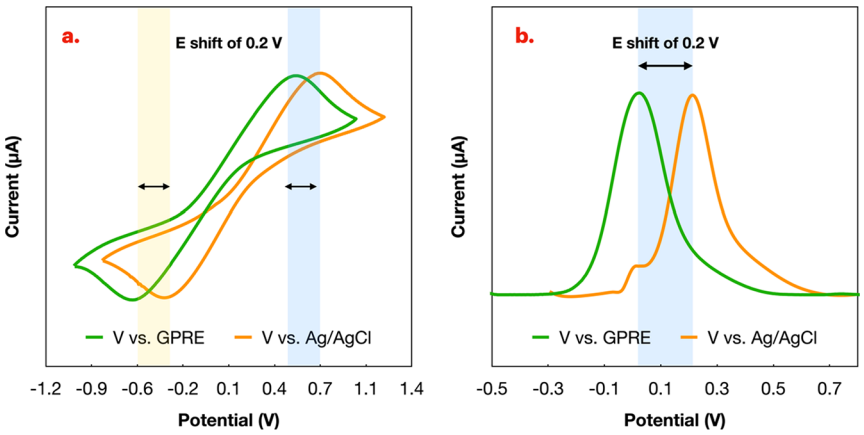

Figure 1. CVs and SWVs of $[Fe(CN)_6]^{3-/4-}$ in 0.5 M KCl using Ag/AgCl RE and GPRE. For CV (a), the potential was scanned from −1.0 to 1.0 V (vs GPRE) and from −0.8 to 1.2 V (vs Ag/AgCl), employing a potential step of 0.01 V and a scan rate of 0.1 V s^{-1} for both systems. In the case of SWV (b), the potential was scanned from −0.5 to 0.8 V (vs GPRE) and from −0.3 to 0.8 V (vs Ag/AgCl), employing a step potential of 5 mV, an amplitude of 0.25 V, and a frequency of 5 Hz (n = 5).

degradation over time, the stability of the Ag/AgCl RE is affected, leading to the loss in the accuracy of the reference potential.[18,19] The stable working time of a commercial Ag/AgCl PRE has been reported to only last for 30 min (for long-term monitoring), which has been attributed to potential drift.[15]

Previously, carbon-based PREs such as graphitic carbon[20−23] or activated carbon[24] have shown promising applications ranging from pH sensing[25] and corrosion monitoring[26] to an ion-sensitive field effect transistor (ISFET)-based sensor,[27] as well as in battery and supercapacitor devices.[28,29] In this regard, our group has been particularly interested in the graphene pseudoreference electrode (GPRE) because the chemical inertness and exceptional resistance (with respect to mechanical stress, temperature change, and ionic interaction) of graphene shed new insights into electrochemical sensing. Unlike Ag/AgCl, graphene exhibits resistance to the above-mentioned factors; as a result, its reference potential remains stable, reducing shifts during experiments. Additionally, while the majority of GPREs have been employed in capacitor and battery applications, only a few have been utilized for sensing applications.[30] One significant advantage of GPRE is the simplicity of its fabrication process. It requires only graphene paste throughout the entire process (in the case of graphene WE/CE/RE), whereas the Ag/AgCl PRE needs a more complex two-step process involving the WE/CE paste and Ag/AgCl component. This streamlined approach speeds up PED production (printing and curing processes), reduces cost, and enhances consistency, especially for large-scale manufacturing. Therefore, this research investigated the capability of GPRE against Ag/AgCl PRE in a PED format.

In advancing the field of electrochemical sensing, this paper introduces a novel GPRE-incorporated PED, which is characterized by its all-graphene composition for the WE, CE, and RE. This unique approach not only paves the way for metal-free sensing systems but also offers enhanced stability and reproducibility in electrochemical measurements compared to systems employing traditional Ag/AgCl PRE. The innovative design of the GPRE-based PED allows for the simultaneous detection of cadmium (Cd) and lead (Pb) and is verified, demonstrating real-world applications. To validate the practical utility of the developed PED, a series of assays in real matrices—including drinking water, wastewater, and biological fluids—are conducted, effectively encompassing diverse applications such as food quality control, environmental monitoring, and medical diagnostics.

2. EXPERIMENTAL SECTION

2.1. Chemical and Apparatus. Details of the chemicals and apparatus can be found in the Supporting Material (SM).

2.2. Electrochemical Measurement. Electrochemical experiments were conducted using an Emstat3 Blue wireless potentiostat (PalmSens BV, The Netherlands). The detection of Cd(II) and Pb(II) was conducted by square-wave anodic stripping voltammetry (SWASV), which was accomplished by transferring 100 μL of a sample solution (or standard Cd(II) and Pb(II)) prepared in a running buffer (comprised of 0.1 M acetate buffer at pH 4.5 along with a Bi(III) standard) onto the designated sample zone. Throughout, the Bi(III) standard concentration was consistently maintained at 10 μg mL^{-1}, which was achieved after the complete dilution of the sample solution or working standard. The detection of Cd(II) and Pb(II) was conducted by SWASV at a potential range of −1.4 to −0.6 V (vs GPRE), unless specified otherwise. Other electrochemical parameters were configured as follows: a step potential of 5 mV (vs GPRE), an amplitude of 0.25 V (vs GPRE), and a frequency of 5 Hz. The optimal deposition potential and duration were −1.6 V (vs GPRE) and 180 s, respectively. Further details of the optimization process are provided in the optimization section in the SM. To investigate the electrochemical characteristics, cyclic voltammogram (CV) curves were recorded by scanning in the voltage range of −1.0 to 1.0 V (vs GPRE). The potential step was set at 0.01 V (vs GPRE), and a scan rate of 0.1 V/s was maintained, unless otherwise specified. All measurements were carried out in three replicas (n = 3).

2.3. Fabrication of the Paper-Based Sensor. The device pattern was created using Adobe Illustrator CC (Adobe Inc., San Jose, California, USA) and printed on Whatman 4 chromatography paper using a wax printer (ColorQube model 8580; Xerox, Connecticut, USA). The printed paper was placed in an oven at 150 °C for 2 min to create a 3D wax barrier. Then, three electrodes (WE, CE, and RE) were screen-printed with the graphene paste onto the wax-printed pattern and dried in an oven at 55 °C for 60 min.[4,31,32] Paper-based sensors were used once and then disposed.

https://doi.org/10.1021/acsomega.3c08249
ACS Omega 2024, 9, 1634−1642

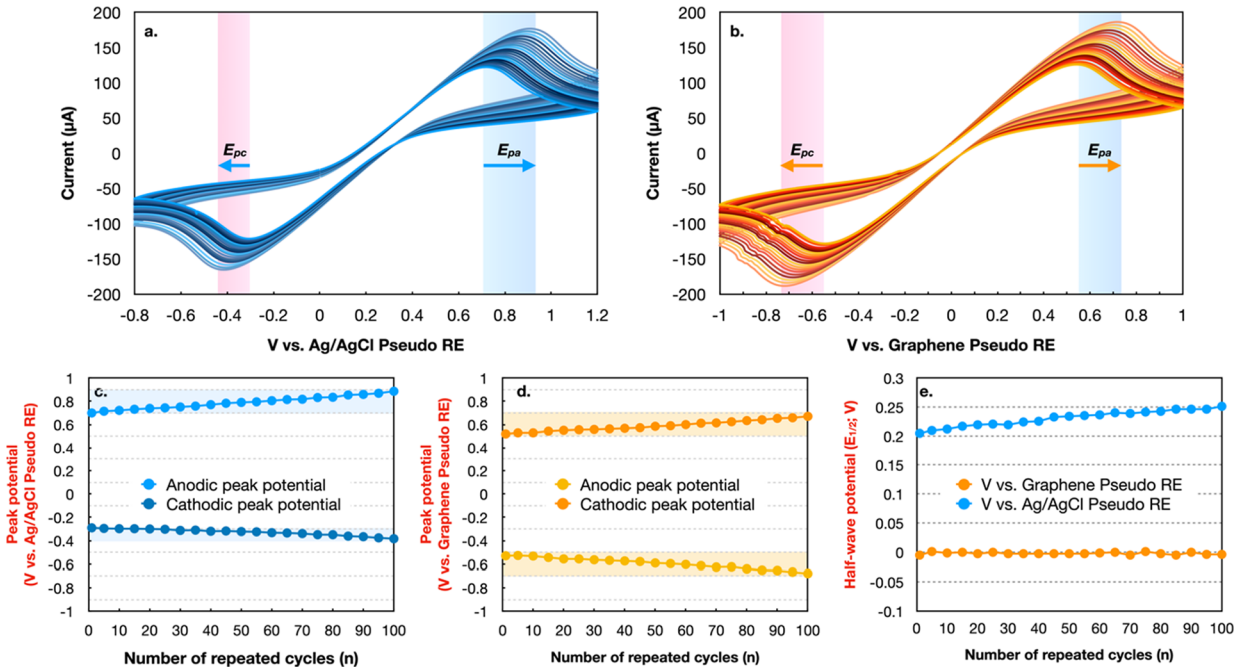

Figure 2. CVs of $[Fe(CN)_6]^{3-/4-}$ in 0.5 M KCl using Ag/AgCl PRE (a) and GPRE (b) for 100 cycles, and their corresponding half-wave potential ($E_{1/2}$) from the obtained CVs (c–e). The CV potential was scanned from −0.8 to 1.2 V (vs Ag/AgCl) and from −1.0 to 1.0 V (vs GPRE), employing a potential step of 0.01 V and a scan rate of 0.1 V s^{-1} for both systems.

2.4. Sample Analysis. Details of the sample analysis can be found in the SM.

2.5. Stability Assessment. Long-term stability was investigated by the accelerated shelf life testing (ASLT) method according to the standard guide for accelerated aging. In this study, the electrodes with the Ag/AgCl PRE and GPRE systems were sealed in an aluminum bag (unless stated otherwise), purged with nitrogen, and placed in an oven at 55 °C. Throughout this process, the half-wave potential ($E_{1/2}$) of each system was monitored continuously by CV, which enabled the calculation and subsequent comparison of the real-time shelf life of the investigated electrodes. The electrochemical species employed for this assessment were 5 mM $[Fe(CN)_6]^{3-/4-}$ and 0.5 M KCl.

3. RESULTS AND DISCUSSION

3.1. Electrochemical Properties of a GPRE. The electrochemical properties of different RE systems, namely, the Ag/AgCl PRE and GPRE, printed onto a paper-based device, were investigated. Figure 1a,b shows the CVs and square-wave voltammograms (SWVs) of 5 mM $[Fe(CN)_6]^{3-/4-}$ in 0.5 M KCl using Ag/AgCl PRE and GPRE. The peak potential of $[Fe(CN)_6]^{3-/4-}$ tested with Ag/AgCl PRE compared to the GPRE is clearly shifted in the negative direction, indicating that the reference potential (E_r) of GPRE is shifted negatively. The CV and SWV data confirm a potential shift of 0.2 V. Notably, a small shoulder peak at 0.0 V vs the Ag/AgCl PRE is observed, particularly under chloride-containing electrolytes (see Figure S1). This oxidation peak is proposed to originate from the introduction of oxidized Ag contaminants during the RE screen printing process or resulting from the corrosion of RE in chloride-containing solutions,[17,33] which also occurs at approximately 0.0 V. These observations suggest that the Ag/AgCl PRE may exhibit limitations in practical electroanalysis owing to its susceptibility to oxidation, leading to reduced durability and reproducibility in various applications.

Next, the electrochemical redox reaction of $[Fe(CN)_6]^{3-/4-}$ in 0.5 M KCl was examined by CV measurements using Ag/AgCl PRE (Figure 2a) and GPRE (Figure 2b) for 100 cycles. Similar CV patterns are observed: the peak potential of the initial CV cycle (first scan) using the GPRE system is shifted negatively by 0.2 V in comparison with that of the initial cycle using the Ag/AgCl PRE. Furthermore, as shown in Figure 2a,b, the peak separation (ΔE) between the anodic peak (E_{pa}) and cathodic peak (E_{pc}) gradually increases and becomes more pronounced after 100 cycles (Figure 2c,d). To quantitatively evaluate the stability of the reference potential, we determined the half-wave potential ($E_{1/2}$) from the obtained CVs. $E_{1/2}$ represents the midpoint between the anodic and cathodic peaks. Interestingly, for the Ag/AgCl PRE under the investigated conditions, $E_{1/2}$ is shifted continuously by approximately 46 mV to positive values after 100 cycles (Figure 2e), indicating its instability for long-term monitoring. The stable working time of the Ag/AgCl PRE has been reported to be approximately 30 min.[18] This potential shift is likely attributed to the cross-contamination between the tested solution (5 mM $[Fe(CN)_6]^{3-/4-}$ in 0.5 M KCl) and the composition of the Ag/AgCl PRE, which is supported by the change in the color of the RE surface from metallic silver to dark brown. Similar results were reported by Lee et al.,[34] suggesting that the Ag/AgCl PRE is not suitable as an RE when significant amounts of redox species are present in an aqueous solution.[35−38] In contrast, $E_{1/2}$ for GPRE remains stable over 100 cycles, indicating its stability and chemical inertness[39] in the tested environment; hence, it is suitable as a PRE.[40] In addition, a chronoamperometric test was performed to monitor the behavior of a redox probe ($[Fe(CN)_6]^{3-/4-}$ in 0.5 M KCl) over time, assessing the real-time stability of the system. A similar trend observed in the CA measurements is described in Figure S2 of Supporting Information. Further

https://doi.org/10.1021/acsomega.3c08249
ACS Omega 2024, 9, 1634−1642

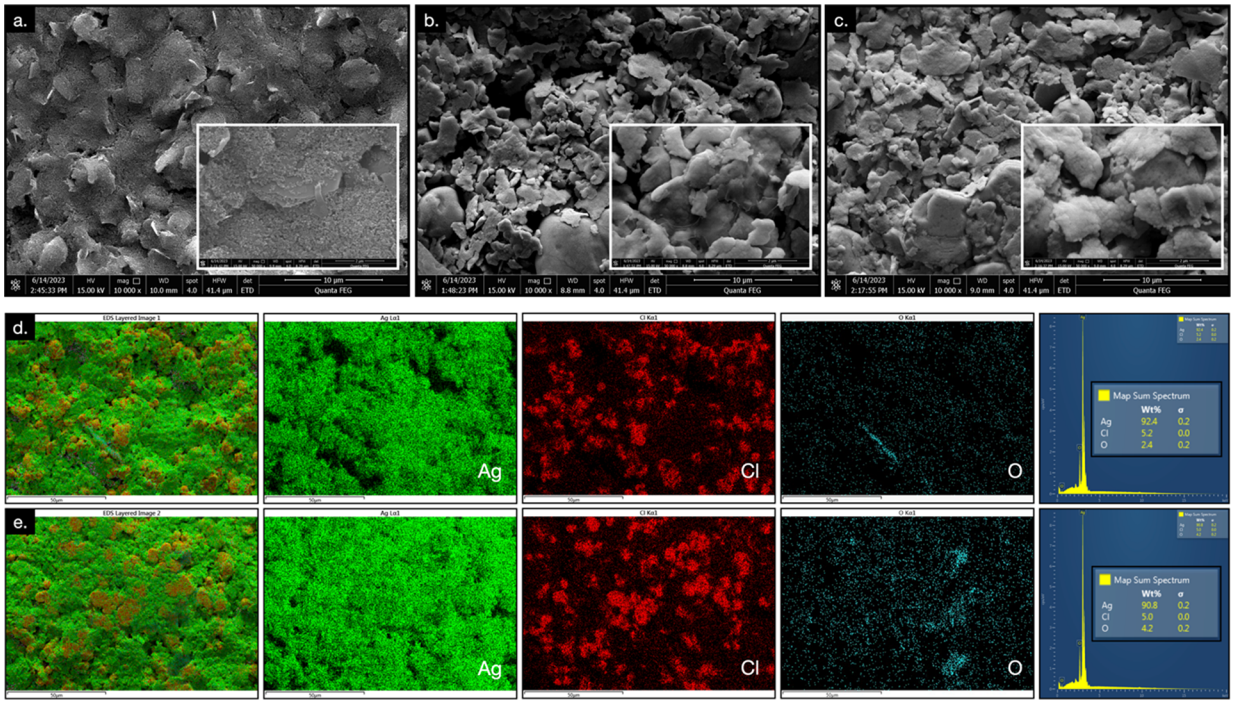

Figure 3. SEM images of GPRE (a), fresh-prepared Ag/AgCl PRE (b), accelerated aging Ag/AgCl PRE (c), and corresponding EDS spectra and elemental mapping of fresh-prepared Ag/AgCl PRE (d) and accelerated aging Ag/AgCl PRE (e).

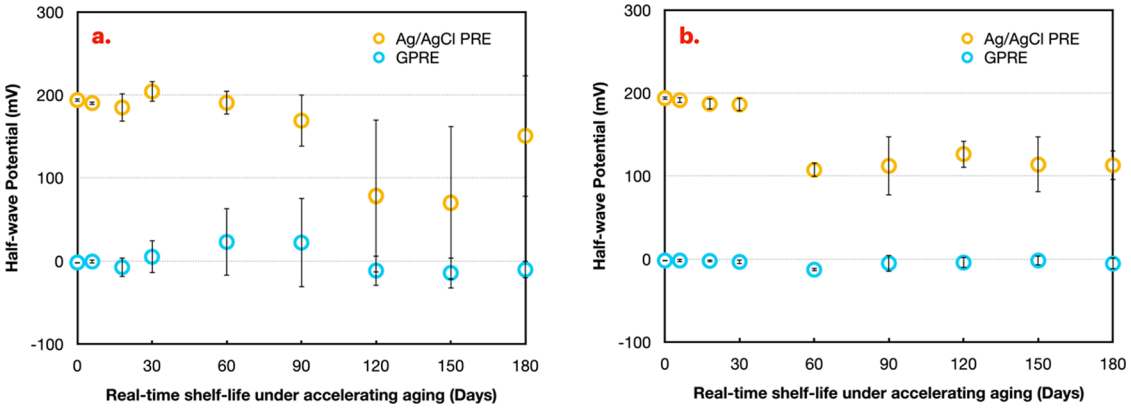

Figure 4. Long-term stability (0−180 days) comparison between GPRE (blue circle) and Ag/AgCl PRE (yellow circle) using ASLT. Left and right compared effects from storage with (a) and without aluminum bags (b). The electrochemical measurements were performed with CV (0.01 V potential step, and 0.1 V s^{-1} scan rate) using 5 mM $[Fe(CN)_6]^{3-/4-}$ in 0.5 M KCl. Standard deviations were represented from triple measurements (n = 3).

discussions of shelf life stability testing are presented in the stability assessment section. Based on these observations, GPRE was selected as the PRE for further investigation.

3.2. Morphological Characterization of GPRE. The morphology of PRE was investigated by scanning electron microscopy (SEM). Figure 3a−c shows the surface morphology of the GPRE and two Ag/AgCl PREs, freshly prepared Ag/AgCl PRE and Ag/AgCl PRE after accelerated aging, respectively. SEM images at 10,000× and 50,000× reveal distinct morphological characteristics of the GPRE and Ag/AgCl PRE. The GPRE exhibits a uniform surface with numerous graphene flakes, while the Ag/AgCl PRE surface is rough and irregular, with abundant particles distributed across its surface. These particles correspond to the AgCl layer formed on the Ag electrode. The uniform GPRE surface is advantageous for achieving stable and consistent electrochemical measurements. Furthermore, the high conductivity of graphene, which is used as the WE and CE, renders efficient charge transfer; as a result, the electrochemical performance is enhanced.

Additionally, the morphologies of the two Ag/AgCl PREs, fresh-prepared Ag/AgCl (Figure 3b) and Ag/AgCl after under accelerated aging, respectively, were examined (Figure 3c). Although the stored Ag/AgCl PREs undergo a change from a shiny silver metallic color to a dark brown over time, no clear difference is observed in the SEM surface morphology. However, energy-dispersive X-ray spectroscopy and elemental mapping shown in Figure 3d,e clearly demonstrate that the oxygen content of the aged Ag/AgCl PRE is almost doubled in comparison with that of the freshly prepared Ag/AgCl PRE (increasing from 2.4 to 4.2 wt%). This result indicates that the Ag/AgCl electrode surface is sensitive to oxygen-rich environ-

https://doi.org/10.1021/acsomega.3c08249
ACS Omega 2024, 9, 1634−1642

ments, which provides additional justification for its limited lifespan. Figure S3a presents an EDX elemental spectrum of the GPRE for a comprehensive comparison. Additional results related to the stability assessment are discussed in a subsequent section.

Additional characterization techniques (transmission electron microscopy (TEM) and confocal laser scanning microscopy (CLSM)) are detailed in Figure S3b−d.

3.3. Long-Term Stability of GPRE. Device stability is a crucial factor in the effective utilization of the sensor. To assess the stability, the long-term stability of the GPRE was compared with that of the Ag/AgCl PRE by ASLT. This method is used to rapidly predict the device's lifespan in the absence of real-time data. In this study, electrodes were subjected to high-temperature stress (55 °C) in an oven for 30 days (accelerated aging time), and the half-wave potential ($E_{1/2}$) of each system was monitored. The real-time shelf life was calculated using the following equation:

$$\text{Real-time shelf life} = \text{Accelerated aging time} \times \text{Reaction rate}^{\text{TE}-\text{TA}/10} \quad (1)$$

where the reaction rate is set to 2, TE represents the evaluation temperature (55 °C), and TA represents the ambient temperature (25 °C). $E_{1/2}$ of the electrode with GPRE is shifted by less than 20 mV throughout the 180 day real-time shelf life accelerated aging study (Figure 4a,b). In contrast, the electrode with the Ag/AgCl PRE exhibits a potential shift of less than 20 mV for only 60 days in a sealed aluminum bag and 30 days in the absence of a sealed aluminum bag. This potential drift observed for the Ag/AgCl PRE can be attributed to mixed potential contributions from reactions involving Ag oxides formed during storage in an oxygen-rich environment.[19] Similar performance characteristics of the printed Ag/AgCl PRE, reflecting a storage life of approximately 30−40 days, also have been reported previously.[18,19] Therefore, the long lifespan and low drift observed with the GPRE provide further evidence of the effectiveness of graphene materials as PREs. Besides stability, cost, and fabrication procedures are also key factors that determine the effectiveness of GPRE. By utilizing GPRE, the cost of the graphene-based paste is significantly reduced (approximately 577 USD/kg) in comparison with that of Ag/AgCl (approximately 2827 USD/kg). Additionally, single-step printing of the electrode further reduces the overall cost and fabrication time. Considering all of these factors, GPRE is an excellent choice to fabricate electrodes. Table 1 summarizes the overall characteristics.

3.4. Application of the GPRE-Incorporated Paper-Based Device for the In Situ Electrochemical Detection of Cd(II) and Pb(II) Using a Bi-Modified Electrode. Heavy metals such as cadmium (Cd) and lead (Pb) pose significant risks to human health, necessitating efficient methods to monitor these metals.[41−44] Owing to their sensitivity and selectivity, electrochemical sensors have been widely used for the detection of heavy metals.[45,46] The anodic stripping voltammetry (ASV) sensor has been extensively employed for the detection of Cd and Pb. When a Cd- or Pb-containing sample is introduced, the metal ions preconcentrate on the WE surface. Next, under the application of an applied voltage, the metal ions from the electrode are stripped and the resulting current is measured, which helps in the determination of the metal ion concentration of the sample. Thus, RE (in this work, PRE) should exhibit stability and a well-defined electrode potential. However, the use of screen-printed Ag/AgCl as a PRE for detecting heavy metals might not be suitable due to its potential drift and the potential environmental impact of silver (Ag). This is important given that silver (Ag), exhibiting a density of 10.49 g/cm^3, is classified as a heavy metal, akin to Cd and Pb. Thus, Cd(II) and Pb(II) could be helpful for studying GPRE behavior against Ag/AgCl PRE. By exploiting the potential of a paper-based device with the GPRE system, the proposed sensor is applied for detecting heavy metals across a range of applications, encompassing environmental monitoring, food quality control, and medical diagnostics.

Table 1. Comparison between Graphene GPRE and Ag/AgCl PRE

factors	Ag/AgCl PRE	GPRE
cost	higher cost (approximately 2827 USD/Kg)	significantly lower cost (approximately 577 USD/kg)
fabrication step	multistep process	single-step printing process
stability	prone to potential shifts and oxidation	excellent stability and chemical inertness
applications	limited to certain applications (not suitable when significant amounts of redox species are present)	versatile applications
environmental impact	environmental concerns	eco-friendly

During the ASV preconcentration step, WE will be codeposited with Bi(III) to facilitate the formation of "fused alloys" with Cd(II) and Pb(II) and promote their deposition on the electrode surface.[47] Figure 5a shows the ASVs for the detection of Cd(II) and Pb(II) at different electrodes, including an in situ Bi(III)-modified electrode and an unmodified electrode. The anodic peaks of Cd(II) and Pb(II) are observed at approximately −1.1 and −0.9 V vs GPRE, respectively. Interestingly, the peaks of Cd(II) and Pb(II) over the unmodified electrode are clearly distinguished, which can be attributed to the abundance of graphene sheets on the electrode surface. However, the presence of Bi(III) significantly enhances the intensity of the peaks for both metals. Notably, Bi(III) can be stripped off at approximately −0.4 V vs GPRE using an in situ Bi-modified electrode, both with or without the presence of Cd(II) and Pb(II). A slight increment (1.2-fold) in the peak current is observed for Pb(II), whereas a remarkable 2.5-fold increment in the peak current is observed for Cd(II). This improvement can be attributed to the role of Bi(III) in promoting a larger electrode surface area and facilitating enhanced metal deposition via the formation of "fused alloys" with Cd(II) and Pb(II).[47]

Subsequently, the simultaneous detection of different concentrations of a mixture of Cd(II) and Pb(II) was conducted by ASV using an in situ Bi-modified electrode (Figure 5b). Under the examined conditions, parallel concentrations (0.1, 0.25, 0.5, 0.75, and 1.0 μg mL^{-1}) of Cd(II) and Pb(II) are simultaneously detected without mutual interference. This result provides strong confirmation of the promising potential of in situ Bi deposition for the simultaneous detection of Cd(II) and Pb(II). To maximize the electrochemical response, various conditions, including deposition time, deposition potential, and Bi(III) concentration, that affect the performance of the sensor were investigated thoroughly. In summary, a deposition time of 180 s, a deposition potential of −1.6 V vs GPRE, and an

https://doi.org/10.1021/acsomega.3c08249
ACS Omega 2024, 9, 1634−1642

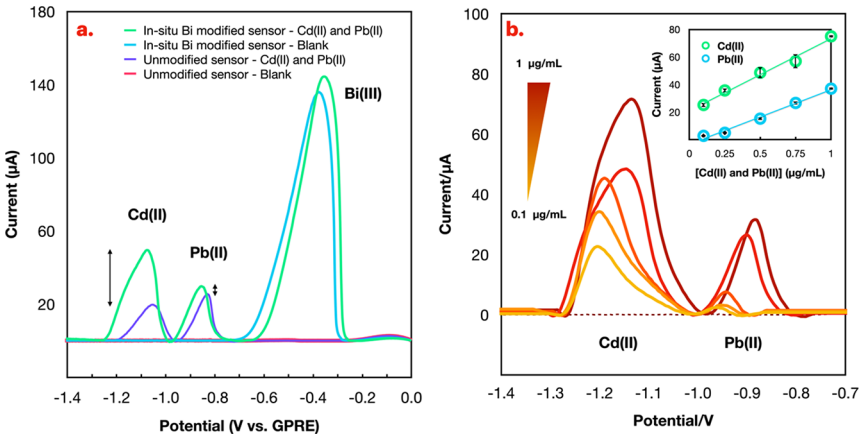

Figure 5. (a) SWASV of a mixture of 0.5 μg mL^{-1} Cd(II) and Pb(II), and blank (acetate buffer pH 4.5) tested with unmodified electrode and in situ Bi(III)-modified electrode (color labels are displayed within the figure) at a potential range of −1.4 to 0.0 V (vs GPRE). (b) SWASVs of Cd(II) and Pb(II) at parallel concentrations of 0.1, 0.25, 0.5, 0.75, and 1 μg mL^{-1} using in situ Bi(III)-modified electrode at a potential range of −1.4 to −0.6 V (vs GPRE) and the inset showing a linear relationship between the anodic peak currents and different Cd(II) and Pb(II) concentrations (n = 3). Other electrochemical parameters were configured as follows: a step potential of 5 mV (vs GPRE), amplitude of 0.25 V (vs GPRE), frequency of 5 Hz, deposition potential of −1.6 V (vs GPRE), and deposition time of 180 s.

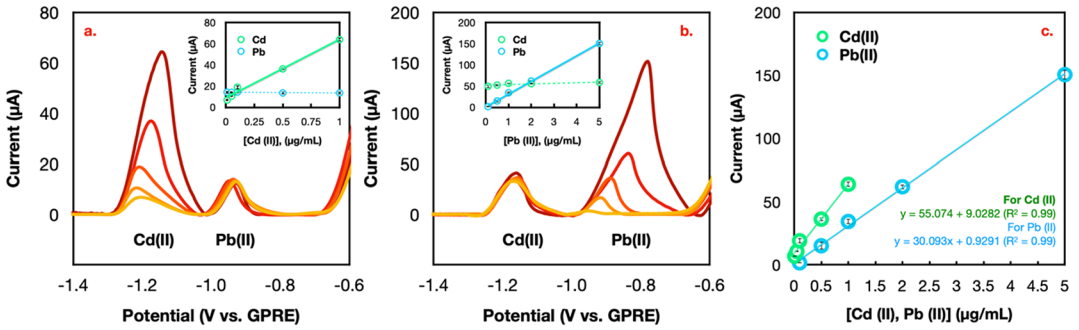

Figure 6. Analytical performance for the detection of Cd(II) and Pb(II). Plots (a) and (b) are SWASVs of Cd(II) and Pb(II) mixtures, where one metal was maintained at a fixed concentration of 0.5 μg mL^{-1} for the detection of another metal, along with its corresponding linear relationship (c) between the anodic peak currents and concentrations of Cd(II) and Pb(II) (n = 4). SWASV was scanned from −1.4 to −0.6 V (vs GPRE) utilizing the following electrochemical parameters: a step potential of 5 mV (vs GPRE), amplitude of 0.25 V (vs GPRE), frequency of 5 Hz, deposition potential of −1.6 V (vs GPRE), and deposition time of 180 s.

optimal Bi(III) concentration of 10 μg mL^{-1} were selected for this study (Figure S4a−c). The supporting material contains details of the assay optimization.

3.5. Analytical Performance. Under the optimized conditions, SWASV was employed to evaluate the analytical performance of GPRE PED for the simultaneous detection of Cd(II) and Pb(II). A solution mixture of Cd(II) and Pb(II) was used, where the concentration of one metal was maintained constant (0.5 μg mL^{-1}) for the detection of another metal. Linear dynamic ranges are established between 0.01 and 1 μg mL^{-1} for Cd(II) and between 0.1 and 5 μg mL^{-1} for Pb(II) with sensitivities of 70.16 and 38.34 μA·mL·μg^{-1}·cm^{-2}, respectively (Figure 6a,b). The limits of detection (LOD) are determined to be 0.69 ng mL^{-1} for Cd(II) and 5.77 ng mL^{-1} for Pb(II), while the limits of quantitation are calculated to be 2.30 ng mL^{-1} for Cd(II) and 19.2 ng mL^{-1} for Pb(II) (calculated as 3 SD_{blank}/slope and 10 SD_{blank}/slope, respectively). Experimentally, the lowest levels of Cd(II) and Pb(II) that could be distinguished from the background noise with a signal-to-noise ratio of 3 were determined to be 3 and 25 ng mL^{-1}, respectively. Furthermore, the LOQs, representing the minimum concentrations at which the analytes could be quantified with acceptable precision and accuracy, were found to be 10 ng mL^{-1} for Cd(II) and 100 ng mL^{-1} for Pb(II). These values were also identified as the starting points of the LDR for each respective metal. The relative standard deviations from the triple measurements of Cd(II) at concentrations of 50 and 500 ng mL^{-1} and Pb(II) at concentrations of 500 and 1000 ng mL^{-1} are less than 5.4% (n = 3), indicative of the reproducibility of the proposed device. Next, the impact of interfering metals (such as Ca(II), Mg(II), Cr(VI), As(III), Sb(III), Fe(II), Fe(III), Zn(II), Ni(II), Hg(II), and Cu(II)) on the developed electrode was investigated further (Figures S5 and S6). The tolerance limit of each metal was in the range of 10- to 50-fold higher than the target ions (500 ng mL^{-1} of Cd(II) and Pb(II)). Details can be found in the SM. The electroanalytical performances of the proposed platforms were compared with those of previous studies and are summarized in Table S1.

3.6. Sample Analysis and Blind Testing. To validate the proposed electrochemical device for the direct determination of Cd(II) and Pb(II) in various sensing applications, different samples from each application were analyzed. Mineral drinking water, industrial wastewater, tap water, seawater, urine, and saliva samples were examined by using the proposed system. The obtained results were compared with those obtained by inductively coupled plasma-mass spectrometry (ICP-MS). Notably, the high salinity of seawater samples can cause salt

https://doi.org/10.1021/acsomega.3c08249
ACS Omega 2024, 9, 1634−1642

precipitation and buildup in the ICP instrument, potentially damaging it. Therefore, these samples (seawater) are analyzed individually and validated by flame atomic absorption spectrophotometry (FAAS), exhibiting limited sensitivity. As shown in Table 2, the data obtained from the proposed

Table 2. Blind Testing Results (n = 10) for the Qualitative, Semiquantitative, and Quantitative Detection Using a Paper-Based Electrochemical Sensor

qualitative detection (n = 10)		
information	Cd	Pb
yes/no	100% (10/10)	100% (10/10)
semiquantitative detection (n = 10)		
information	Cd	Pb
high (1000 ng mL^{-1})	100% (10/10)	100% (10/10)
medium (500 ng mL^{-1})	90% (9/10)	80% (8/10)
low (250 ng mL^{-1})	100% (10/10)	100% (10/10)
quantitative detection (n = 10)		
information	Cd	Pb
correlation coefficient (R^2)	0.9999	0.9996
slope	0.9345	0.9622

method and standard methods do not reveal any significant difference between the two approaches (paired t test at a 95% confidence interval reveals that the experimental t values (t calculated values are 0.12 for Cd(II) and 1.20 for Pb(II)) are less than the t critical values (1.79 for Cd(II) and 1.78 for Pb(II)). This demonstrates the applicability and reliability of the proposed approach. Additionally, recovery tests were conducted by spiking the samples with Cd(II) and Pb(II) at concentration levels of 100 and 500 ng mL^{-1}. The data listed in Table S2 also reveal that the overall percentage recoveries (80.9−108%) fall within the acceptable range[48] (between 80 and 110%), indicating the proficiency of the method for detecting Cd(II) and Pb(II) in such samples.

In this study, a PED is proposed as an innovative tool for the portable simultaneous determination of Cd(II) and Pb(II) by untrained personnel. To test this hypothesis, 10 randomly selected high-school students (grade 12) from Kamnoetvidya Science Academy, who had no prior experience using this device, were selected to perform the entire electrochemical assay and evaluate the results at three levels of interpretation: qualitative, semiquantitative, and quantitative. A structural guideline was provided for their evaluation. For qualitative interpretation, the presence or absence of peaks corresponding to the metal in the voltammogram was assessed. All 10 users (100%) identified the presence of both metals. For semiquantitative interpretation, three blind concentrations of Cd(II) and Pb(II) were investigated. The data were interpreted by comparing the obtained peak current (peak height) to the standard calibration plot prepared by the author. All users (100%) accurately distinguished between low and high levels of Cd(II) and Pb(II), while some users misinterpreted the medium level of Cd(II) and Pb(II) (90 and 80% of users accurately distinguished the levels of Cd(II) and Pb(II)). For quantitation, the linear calibration plot obtained by all of the users was compared with that prepared by the author. A strong positive correlation was observed between the peak currents obtained from trained and untrained users (Table 2 and Figure S7a,b). These results suggest that the proposed device can be effectively used, even by untrained users.

4. CONCLUSIONS

In this study, a GPRE is integrated into a PED, and the developed GPRE-based PED is applied for the sensitive and selective detection of heavy metals, viz. Cd and Pb, by ASV. The performance and stability of GPRE in comparison with those of traditional Ag/AgCl PRE are highlighted. The results demonstrate that GPRE exhibits chemical inertness, stability, and reproducible potentials in electrochemical measurements, overcoming the limitations of traditional Ag/AgCl such as potential shifts in the presence of interacting ions, inaccuracies in dynamic environments, and notably, its poor stability and limited operational lifespan. The developed GPRE-based PED demonstrates robust analytical performance, including a wide linear range, low LOD, and acceptable sensitivity; hence, it is suitable for real-world applications. The proposed sensor is successfully employed for the analysis of various samples, demonstrating its practical utility. Notably, the accessibility of the sensor is confirmed by its effective use by untrained users. By addressing the aforementioned limitations of the Ag/AgCl PRE, our study positions the GPRE as a transformative solution, enhancing the applicability of paper-based electrochemical sensors. The results underscore the immense potential of a GPRE-equipped PED not only for the accurate detection of heavy metals but also for broader applications, marking a significant advancement in the field.

■ ASSOCIATED CONTENT

Supporting Information

The Supporting Information is available free of charge at https://pubs.acs.org/doi/10.1021/acsomega.3c08249.

Effect of background electrolyte on Ag/AgCl PRE; real-time monitoring of electrode stability; additional morphological characterizations; assay optimization; interference study; blind testing; comparison of the presented method with other electrochemical sensors for the Cd (II) and Pb (II) determination; and recovery tests of GPRE PED and conventional methods (ICP-MS and FAAS) (PDF)

■ AUTHOR INFORMATION

Corresponding Author

Abdulhadee Yakoh − *The Institute of Biotechnology and Genetic Engineering and Center of Excellence for Food and Water Risk Analysis (FAWRA), Department of Veterinary Public Health, Faculty of Veterinary Science, Chulalongkorn University, Bangkok 10330, Thailand;* orcid.org/0000-0002-8392-5492; Email: Abdulhadee.y@chula.ac.th

Authors

Prasongporn Ruengpirasiri − *Kamnoetvidya Science Academy, Rayong 21210, Thailand*

Pimchanok Charoensin − *Kamnoetvidya Science Academy, Rayong 21210, Thailand*

Akkrawat Aniwattapong − *Kamnoetvidya Science Academy, Rayong 21210, Thailand*

Pemika Natekuekool − *Kamnoetvidya Science Academy, Rayong 21210, Thailand*

https://doi.org/10.1021/acsomega.3c08249
ACS Omega 2024, 9, 1634−1642

Chawin Srisomwat − *Department of Chemistry, Faculty of Science and Technology, Thammasat University, Pathumthani 12121, Thailand*

Chanika Pinyorospathum − *National Laboratory Animal Center, Mahidol University, Nakhon Pathom 73170, Thailand; Analytical Sciences and National Doping Test Institute, Mahidol University, Bangkok 10400, Thailand*

Sudkate Chaiyo − *The Institute of Biotechnology and Genetic Engineering and Center of Excellence for Food and Water Risk Analysis (FAWRA), Department of Veterinary Public Health, Faculty of Veterinary Science, Chulalongkorn University, Bangkok 10330, Thailand;* orcid.org/0000-0002-4527-7041

Complete contact information is available at: https://pubs.acs.org/10.1021/acsomega.3c08249

Notes

The authors declare no competing financial interest.

■ ACKNOWLEDGMENTS

Financial support for this research was obtained from the Chulalongkorn University for the development of new faculty staff and Thailand Science research and Innovation Fund Chulalongkorn University.

■ REFERENCES

(1) Batista deroco, P.; Giarola, J. d. F.; Wachholz júnior, D.; Arantes lorga, G.; Tatsuo kubota, L. Chapter Four - Paper-based electrochemical sensing devices. In *Comprehensive Analytical Chemistry*; Merkoçi, A., Ed.; Elsevier, 2020; vol *89*, pp 91−137.

(2) Noviana, E.; Mccord, C. P.; Clark, K. M.; Jang, I.; Henry, C. S. Electrochemical paper-based devices: sensing approaches and progress toward practical applications. *Lab on a Chip* **2020**, *20* (1), 9−34.

(3) Bordbar, M. M.; Sheini, A.; Hashemi, P.; Hajian, A.; Bagheri, H. Disposable Paper-Based Biosensors for the Point-of-Care Detection of Hazardous Contaminations—A Review. *Biosensors* **2021**, *11*, 316 DOI: 10.3390/bios11090316.

(4) Yakoh, A.; Pimpitak, U.; Rengpipat, S.; Hirankarn, N.; Chailapakul, O.; Chaiyo, S. Paper-based electrochemical biosensor for diagnosing COVID-19: Detection of SARS-CoV-2 antibodies and antigen. *Biosensors and Bioelectronics* **2021**, *176*, No. 112912.

(5) Srisomwat, C.; Teengam, P.; Chuaypen, N.; Tangkijvanich, P.; Vilaivan, T.; Chailapakul, O. Pop-up paper electrochemical device for label-free hepatitis B virus DNA detection. *Sensors and Actuators B: Chemical* **2020**, *316*, No. 128077.

(6) Costa-Rama, E.; Fernández-Abedul, M. T. Paper-Based Screen-Printed Electrodes: A New Generation of Low-Cost Electroanalytical Platforms. *Biosensors* **2021**, *11*, 51 DOI: 10.3390/bios11020051.

(7) Sun, Y.; Jiang, Q.-Y.; Chen, F.; Cao, Y. Paper-based electrochemical sensor. *Electrochem. Sci. Adv.* **2022**, *2* (4), No. e2100057.

(8) Laschi, S.; Mascini, M. Planar electrochemical sensors for biomedical applications. *Medical Engineering & Physics* **2006**, *28* (10), 934−943.

(9) Metters, J. P.; Kadara, R. O.; Banks, C. E. New directions in screen printed electroanalytical sensors: an overview of recent developments. *Analyst* **2011**, *136* (6), 1067−1076.

(10) Foster, C. W.; Kadara, R. O.; Banks, C. E., Fundamentals of Screen-Printing Electrochemical Architectures. In *Screen-Printing Electrochemical Architectures*; Springer International Publishing: Cham, 2016; pp 13−23.

(11) Paimard, G.; Ghasali, E.; Baeza, M. Screen-Printed Electrodes: Fabrication, Modification, and Biosensing Applications. *Chemosensors* **2023**, *11*, 113 DOI: 10.3390/chemosensors11020113.

(12) García-miranda ferrari, A.; Rowley-neale, S. J.; Banks, C. E. Screen-printed electrodes: Transitioning the laboratory in-to-the field. *Talanta Open* **2021**, *3*, No. 100032.

(13) Carvalho, J. H. S.; Gogola, J. L.; Bergamini, M. F.; Marcolino-junior, L. H.; Janegitz, B. C. Disposable and low-cost lab-made screen-printed electrodes for voltammetric determination of L-dopa. *Sensors and Actuators Reports* **2021**, *3*, No. 100056.

(14) Couto, R. A. S.; Lima, J. L. F. C.; Quinaz, M. B. Recent developments, characteristics and potential applications of screen-printed electrodes in pharmaceutical and biological analysis. *Talanta* **2016**, *146*, 801−814.

(15) Sophocleous, M.; Atkinson, J. K. A review of screen-printed silver/silver chloride (Ag/AgCl) reference electrodes potentially suitable for environmental potentiometric sensors. *Sensors and Actuators A: Physical* **2017**, *267*, 106−120.

(16) Inzelt, G. Pseudo-reference Electrodes. In *Handbook of Reference Electrodes*; Inzelt, G.; Lewenstam, A.; Scholz, F., Eds.; Springer Berlin Heidelberg: Berlin, Heidelberg, 2013; pp 331−332.

(17) Dawkins, R. C.; Wen, D.; Hart, J. N.; Vepsäläinen, M. A screen-printed Ag/AgCl reference electrode with long-term stability for electroanalytical applications. *Electrochim. Acta* **2021**, *393*, No. 139043.

(18) Sun, J.; Wang, Q.; Luo, G.; Meng, W.; Cao, M.; Li, Y.; Masterman-smith, M. D.; Yang, H.; Sun, X.; Lang, M.-F. A novel flexible Ag/AgCl quasi-reference electrode based on silver nanowires toward ultracomfortable electrophysiology and sensitive electrochemical glucose detection. *Journal of Materials Research and Technology* **2020**, *9* (6), 13425−13433.

(19) Søpstad, S.; Johannessen, E. A.; Seland, F.; Imenes, K. Long-term stability of screen-printed pseudo-reference electrodes for electrochemical biosensors. *Electrochim. Acta* **2018**, *287*, 29−36.

(20) Honeychurch, K. C.; Rymansaib, Z.; Iravani, P. Anodic stripping voltammetric determination of zinc at a 3-D printed carbon nanofiber−graphite−polystyrene electrode using a carbon pseudo-reference electrode. *Sensors and Actuators B: Chemical* **2018**, *267*, 476−482.

(21) Chaiyo, S.; Mehmeti, E.; Siangproh, W.; Hoang, T. L.; Nguyen, H. P.; Chailapakul, O.; Kalcher, K. Non-enzymatic electrochemical detection of glucose with a disposable paper-based sensor using a cobalt phthalocyanine−ionic liquid−graphene composite. *Biosensors and Bioelectronics* **2018**, *102*, 113−120.

(22) Pollok, N. E.; Peng, Y.; Rabin, C.; Richards, I.; Crooks, R. M. Effect of Serum on Electrochemical Detection of Bioassays Having Ag Nanoparticle Labels. *ACS Sensors* **2021**, *6* (5), 1956−1962.

(23) Fernandes, J. C. B.; Heinke, E. V. Alternative strategy for manufacturing of all-solid-state reference electrodes for potentiometry. *J. Sens. Sens. Syst.* **2015**, *4* (1), 53−61.

(24) Abbas, Y.; Pargar, F.; Olthuis, W.; Van den berg, A. Activated Carbon as a Pseudo-reference Electrode for Potentiometric Sensing Inside Concrete. *Procedia Engineering* **2014**, *87*, 1437−1440.

(25) Kim, D. H.; Park, W. H.; Oh, H. G.; Jeon, D. C.; Lim, J. M.; Song, K. S. Two-Channel Graphene pH Sensor Using Semi-Ionic Fluorinated Graphene Reference Electrode. *Sensors* **2020**, *20*, No. 4184, DOI: 10.3390/s20154184.

(26) Jin, M.; Jiang, Y.; Jiang, L.; Chu, H.; Zhi, F.; Gao, S. Fabrication and characterization of pseudo reference electrode based on graphene-cement composites for corrosion monitoring in reinforced concrete structure. *Construction and Building Materials* **2019**, *204*, 144−157.

(27) Tintelott, M.; Kremers, T.; Ingebrandt, S.; Pachauri, V.; Vu, X. T. Realization of a PEDOT:PSS/Graphene Oxide On-Chip Pseudo-Reference Electrode for Integrated ISFETs. *Sensors* **2022**, *22*, No. 2999, DOI: 10.3390/s22082999.

(28) Liu, X.; Elia, G. A.; Passerini, S. Evaluation of counter and reference electrodes for the investigation of Ca battery materials. *Journal of Power Sources Advances* **2020**, *2*, No. 100008.

(29) Widmaier, M.; Krüner, B.; Jäckel, N.; Aslan, M.; Fleischmann, S.; Engel, C.; Presser, V. Carbon as Quasi-Reference Electrode in Unconventional Lithium-Salt Containing Electrolytes for Hybrid

Battery/Supercapacitor Devices. *Journal of The Electrochemical Society* **2016**, *163* (14), A2956.
(30) Costa, W. R. P.; Rocha, R. G.; De faria, L. V.; Matias, T. A.; Ramos, D. L. O.; Dias, A. G. C.; Fernandes, G. L.; Richter, E. M.; Muñoz, R. A. A. Affordable equipment to fabricate laser-induced graphene electrodes for portable electrochemical sensing. *Microchim. Acta* **2022**, *189* (5), 185.
(31) Yakoh, A.; Chaiyo, S.; Siangproh, W.; Chailapakul, O. 3D Capillary-Driven Paper-Based Sequential Microfluidic Device for Electrochemical Sensing Applications. *ACS Sensors* **2019**, *4* (5), 1211−1221.
(32) Cate, D. M.; Adkins, J. A.; Mettakoonpitak, J.; Henry, C. S. Recent Developments in Paper-Based Microfluidic Devices. *Anal. Chem.* **2015**, *87* (1), 19−41.
(33) Russo, L.; Leva bueno, J.; Bergua, J. F.; Costantini, M.; Giannetto, M.; Puntes, V.; De la escosura-muñiz, A.; Merkoçi, A. Low-Cost Strategy for the Development of a Rapid Electrochemical Assay for Bacteria Detection Based on AuAg Nanoshells. *ACS Omega* **2018**, 3 (12), 18849−18856.
(34) Lee, J.; Jäckel, N.; Kim, D.; Widmaier, M.; Sathyamoorthi, S.; Srimuk, P.; Kim, C.; Fleischmann, S.; Zeiger, M.; Presser, V. Porous carbon as a quasi-reference electrode in aqueous electrolytes. *Electrochim. Acta* **2016**, *222*, 1800−1805.
(35) Senthilkumar, S. T.; Selvan, R. K.; Melo, J. S. Redox additive/active electrolytes: a novel approach to enhance the performance of supercapacitors. *Journal of Materials Chemistry A* **2013**, *1* (40), 12386−12394.
(36) Fic, K.; Meller, M.; Frackowiak, E. Interfacial Redox Phenomena for Enhanced Aqueous Supercapacitors. *Journal of The Electrochemical Society* **2015**, *162* (5), A5140.
(37) Akinwolemiwa, B.; Peng, C.; Chen, G. Z. Redox Electrolytes in Supercapacitors. *Journal of The Electrochemical Society* **2015**, *162* (5), A5054.
(38) Krüner, B.; Lee, J.; Jäckel, N.; Tolosa, A.; Presser, V. Sub-micrometer Novolac-Derived Carbon Beads for High Performance Supercapacitors and Redox Electrolyte Energy Storage. *ACS Applied Materials & Interfaces* **2016**, *8* (14), 9104−9115.
(39) Liao, L.; Peng, H.; Liu, Z. Chemistry Makes Graphene beyond Graphene. *J. Am. Chem. Soc.* **2014**, *136* (35), 12194−12200.
(40) Ponnuswamy, T.; Chen, J.-J.; Xu, F.; Chyan, O. Monitoring metal ion contamination onset in hydrofluoric acid using silicon−diamond and dual silicon sensing electrode assembly. *Analyst* **2001**, *126* (6), 877−880.
(41) Yantasee, W.; Lin, Y.; Hongsirikarn, K.; Fryxell, G. E.; Addleman, R.; Timchalk, C. Electrochemical Sensors for the Detection of Lead and Other Toxic Heavy Metals: The Next Generation of Personal Exposure Biomonitors. *Environmental Health Perspectives* **2007**, *115* (12), 1683−1690.
(42) Samejo, S.; Baig, J. A.; Uddin, S.; Kazi, T. G.; Afridi, H. I.; Hol, A.; Ali, F. I.; Hussain, S.; Akhtar, K.; Perveen, S.; Bhutto, A. A. Green synthesis of iron oxide nanobiocomposite for the adsorptive removal of heavy metals from the drinking water. *Mater. Chem. Phys.* **2023**, *303*, No. 127807.
(43) Baloch, S.; Kazi, T. G.; Baig, J. A.; Afridi, H. I.; Arain, M. B. Occupational exposure of lead and cadmium on adolescent and adult workers of battery recycling and welding workshops: Adverse impact on health. *Science of The Total Environment* **2020**, *720*, No. 137549.
(44) Junejo, S. H.; Baig, J. A.; Kazi, T. G.; Afridi, H. I. Cadmium and Lead Hazardous Impact Assessment of Pond Fish Species. *Biological Trace Element Research* **2019**, *191* (2), 502−511.
(45) Sajjan, V. A.; Aralekallu, S.; Nemakal, M.; Palanna, M.; Prabhu, C. P. K.; Sannegowda, L. K. Nanomolar detection of lead using electrochemical methods based on a novel phthalocyanine. *Inorg. Chim. Acta* **2020**, *506*, No. 119564.
(46) Palanna, M.; Aralekallu, S.; Keshavananda prabhu, C. P.; Sajjan, V. A.; Mounesh; Sannegowda, L. K. Nanomolar detection of mercury(II) using electropolymerized phthalocyanine film. *Electrochim. Acta* **2021**, *367*, No. 137519.
(47) Chaiyo, S.; Mehmeti, E.; Žagar, K.; Siangproh, W.; Chailapakul, O.; Kalcher, K. Electrochemical sensors for the simultaneous determination of zinc, cadmium and lead using a Nafion/ionic liquid/graphene composite modified screen-printed carbon electrode. *Anal. Chim. Acta* **2016**, *918*, 26−34.
(48) González, A. G.; Herrador, M. Á.; Asuero, A. G. Intra-laboratory assessment of method accuracy (trueness and precision) by using validation standards. *Talanta* **2010**, *82* (5), 1995−1998.

https://doi.org/10.1021/acsomega.3c08249
ACS Omega 2024, 9, 1634−1642